COMPARISON OF DISLOCATION DENSITIES OF PRIMARY AND SECONDARY RECRYSTALLIZATION GRAINS OF Si-Fe*

C. G. DUNNt and E. F. KOCHt

Single crystals of Si-Fe (3 $\frac{1}{4}$ per cent Si) were cold-rolled and annealed to obtain both primary and secondary recrystallization structures. The dislocation densities of the primary and secondary recrystallization grains were measured by an etch-pit method, which also disclosed considerable variation in etch-pit density among the primaries and in many instances within individual primaries. The average dislocation densities were 2×10^7 lines/cm² for primaries and 2×10^6 lines/cm² for secondaries, which indicates that primaries on the average are less perfect than secondaries.

The effects of the observed difference in dislocation density on the driving force for growth in the initial and also in the later stages of secondary recrystallization were considered. Calculations indicate a critical size for growth of a grain in deviating orientation which is substantially above the average size of primaries. The difference in dislocation density contributes approximately 8 per cent to the driving force of a large secondary in the Si-Fe studied.

COMPARISON DES DENSITES DE DISLOCATIONS AU COURS DE LA RECRISTALLISATION PRIMAIRE ET SECONDAIRE DE GRAINS DE Fe-Si

Des monocristaux de Fe-Si (3,25% Si) ont été laminés à froid puis recuits pour provoquer à la fois les structures de recristallisation primaire et secondaire. Les densités de dislocations des grains de recristallisation primaire et secondaire ont été mesurées par la méthode des piqûres de corrosion, qui par ailleurs montre des variations importantes de la densité des piqûres entre les grains de recristallisation primaire et souvent aussi au sein d'un même grain.

Les densités moyennes de dislocations sont de 2.10° lignes/cm² pour les grains primaires et 2.10° lignes/cm² pour les secondaries, ce qui permet de conclure à l'imperfection moyenne plus grande des cristaux primaires. Les auteurs ont observé les effets de la différence en densité de dislocations sur la valeur de la force nécessaire à la croissance au cours des stades initiaux et finaux de la recristallisation secondaire. Les calculs indiquent que la taille critique de croissance d'un grain dont l'orientation diffère de la moyenne, est notablement supérieure à la taille moyenne des grains primaires.

Dans les alliages Fe-Si étudiés la différence de densité de dislocations intervient approximativement pour 8 % dans la valeur de la force nécessaire à la croissance d'un grain secondaire important.

VERGLEICH DER VERSETZUNGSDICHTEN PRIMÄR UND SEKUNDÄR REKRISTALLISIERTER KÖRNER IN SILIZIUM-EISEN

Einkristalle aus Silizium-Eisen $(3\frac{1}{4}\%\,\mathrm{Si})$ wurden kaltgewalzt und geeigneten Glühbehandlungen unterworfen, um sowohl primär als auch sekundar rekristallisiertes Gefüge zu erhalten. Die Versetzungsdichten der primär und der sekundar rekristallisierten Körner wurden mit einem Ätzgrübehen-Verfahren gemessen. Dabei stellten sich heraus, daß die Ätzgrübehendichte zeischen verschiedenen primär kristallisierten Körnern und in manchen Fällen selbst innerhalb ein und desselben Korns beträchtlich schwankt. Als mittlere Versetzungsdichten wurden 2.10° Linien/em-für primär und 2.10° Linien/em-für sekundar rekristallisierte Körner ermittelt, woraus hervorgeht, daß die primär rekristallisierten im Mittel weniger perfekt sind als die sekundär rekristallisierten.

Die Einflüsse der heobachteten Unterschiede in der Versetzungsdichte auf die treibende Kraft des Kornwachstums zu Beginn und auch in den späteren Stadien der sekundären Rekristallisation werden erörtert. Berechnungen ergeben eine kritische Größe für das Washstum eines Korns mit abweichender Orientierung, die wesentlich größer als der mittlere Durchmesser der primären Körner ist. Der Unterschied in der Versetzungsdichte liefert einen Beitrag von etwa 8% zur treibenden Kraft eines großen sekundären Korns in dem hier untersuchten Silizium-Eisen.

INTRODUCTION

Under suitable conditions, certain polycrystalline metals or alloys and also single crystal materials can be cold-rolled and recrystallized to obtain sharp textures and fine-grained structures.^(1, 2) When such materials are annealed further at high temperatures,

they recrystallize again, but to coarse-grained structures. These phenomena are called primary and secondary recrystallization respectively, and the grains produced are called primaries and secondaries. Theories on secondary recrystallization have been advanced; (1, 3, 4, 5) that of Rathenau and Custers (6) considers that the internal state of secondaries is more perfect than the internal state of primaries. Guinier and Tennevin (7) examined Ni-Fe samples used by

^{*} Received March 21, 1957.

[†] General Electric Research Laboratory, Schenectady, New York

Rathenau and Custers and found, however, no difference in the perfection of primaries and secondaries, their method of focusing X-rays at a large distance providing an accuracy of 15 sec of arc in the orientation spread of reflecting plane normals.

In the present investigation an etch-pit technique, which Hibbard and Dunn⁽⁸⁾ found satisfactory for revealing the sites of individual edge dislocations, was used to obtain data on the density of dislocations within primaries and secondaries of Si-Fe samples. The results to be described show that primaries have the higher dislocation density and, therefore, are the less perfect of the two kinds of grains. Calculations are also made to determine the effect of the imperfections on secondary recrystallization.

EXPERIMENTAL PROCEDURE

Original stock for obtaining primary and secondary recrystallization structures consisted of suitably oriented single crystals of silicon-iron (3.25 per cent Si). The crystals were grown to predetermined orientations by the strain-anneal method, using a hydrogen-atmosphere high-temperature-gradient furnace of 1200°C maximum temperature. The orientations of the five crystals used in the present work are listed in Table 1. All crystals were cold-rolled to a reduction in thickness of 70 per cent.

In a number of separate experiments it had been found that the carbon concentration in as-grown crystals was probably under 0.001 per cent and was too low, based on tests and the work of Suits and Low, (9) for the proper application of the etch-pit method. Suits and Low found that a certain amount of carbon is required if etch pits are to form at the sites of edge dislocations during electroetching in a chrome acetic acid bath. A suitable level of carbon, namely, about 0.004 per cent, was introduced into each specimen by heating to 770°C or to a higher tempera-

ture in a measured quantity of low-pressure acetylene. In order to determine whether the carbon addition had any significant effect on the perfection of the primaries and secondaries being studied, the manner of adding the carbon was varied (Table 1), being introduced either before the cold-rolling or at a subsequent point. The treatment for crystal No. 5 was 30 min in low-pressure acetylene at 770°C after the primary recrystallization structure had formed at 980°C.

Although the annealing treatments changed the worked single-crystal structures into fine-grained polycrystalline structures, a separate confirmation of recrystallization was made using X-rays. The X-ray method also showed a complete change in the texture. Table 1 lists the annealing treatments for primary recrystallization. Secondary recrystallization was obtained by annealing at 980°C for prolonged periods of time.

RESULTS

Figs. 1 to 7 show a number of microstructures after primary recrystallization. The primaries have well-defined boundaries and, according to ASTM grain-size standards, have an average diameter of approximately 30 μ . There are etch pits within the primaries, and these are taken to indicate the presence of edge dislocations. Also considerable variation in etch-pit density occurs within individual primaries; so the observed dislocation density of any given primary must be viewed only as part of the three-dimensional structure.

The manner of adding the carbon to obtain etch pits provided the following information. The series shown in Figs. 1–3 for crystal No. I reveals no effect due to temperature of recrystallization. Fig. 4 for crystal No. 2 shows substantially the same structure as crystal No. I, but here the cold-rolling was done on a low-carbon crystal, the carbon being added during the anneal. Figs. 1, 5, and 6, for differently oriented

Table 1. Initial crystal orientation, manner of adding the carbon, and annealing treatment to obtain the primary recrystallization structure

Crystal	Initial orientation		Carbon addition	Annealing treatment
	Rolling plane	Rolling direction		
1 1 1 2 3 4 5	110 110 110 110 332 350 332	100 100 100 100 113 100 113	Before cold-rolling Before cold-rolling Before cold-rolling During annealing treatment Before cold-rolling Before cold-rolling Subsequent to annealing treatment	I min 980° (vacuum) 1 min 900° (vacuum) 35 min 770° (vacuum) 1 min 980°C (low-pressure acetylene) 1 min 980°C (vacuum) 1 min 980°C (vacuum) 1 min 980°C (vacuum)

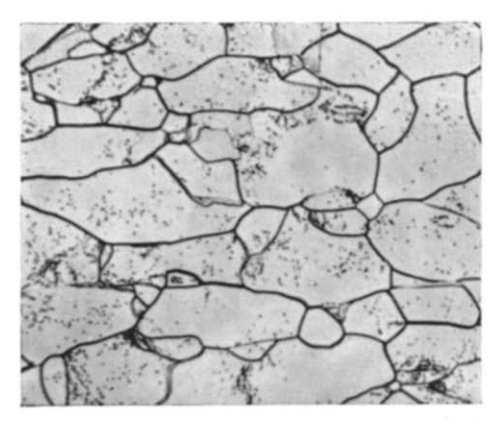


Fig. 1. Microstructure of crystal No. 1 after a 1 min anneal at 980°C. Chrome acetic acid electroetch. \times 500.

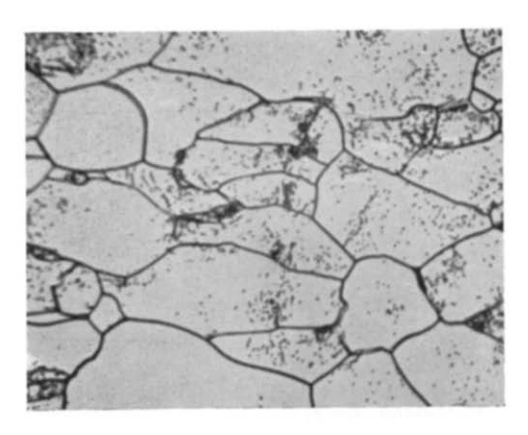


Fig. 4. Microstructure of crystal No. 2 after a 1 min anneal at 980°C. Carbon added during anneal. $\times 500.$

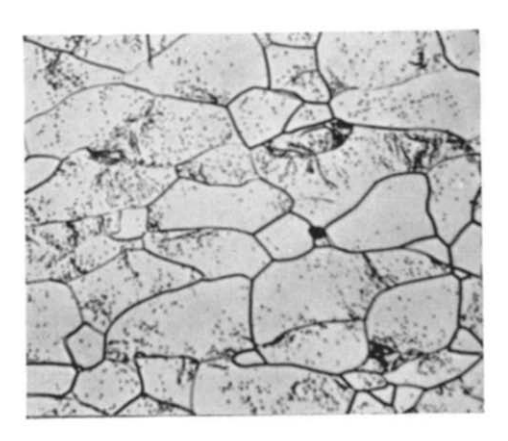


Fig. 2. Microstructure of crystal No. 1 after a 1 min anneal at 900 °C. \times 500.

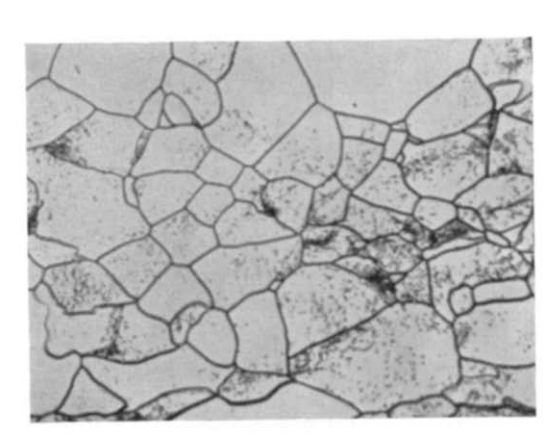


Fig. 5. Microstructure of crystal No. 3 after a 1 min anneal at 980 °C. $\times 500$.

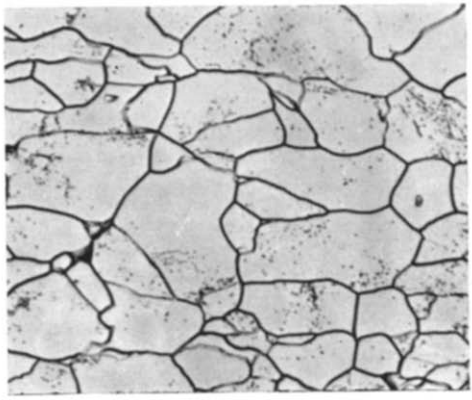


Fig. 3. Microstructure of crystal No. 1 after a 35 min anneal at 770°C. $\times 500.$

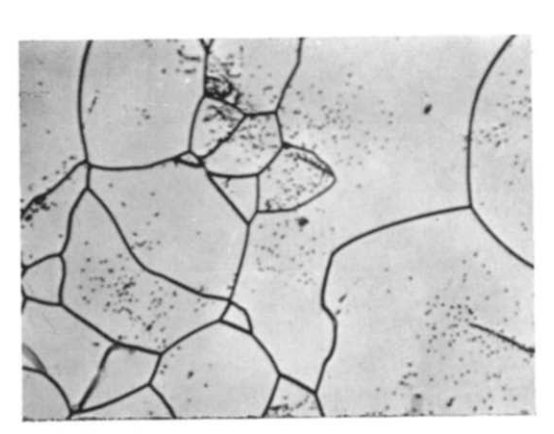


Fig. 6. Microstructure of crystal No. 4 after a 1 min anneal at 980°C. ×500.

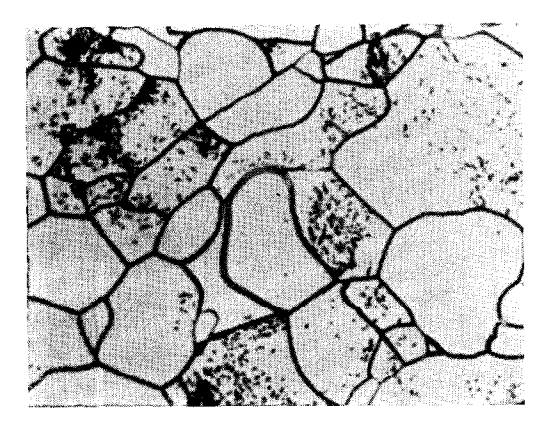


Fig. 7. Microstructure of crystal No. 5 after a 1 min anneal at 980°C and a carbon addition treatment at 770°C. \times 500.

original crystals, show no marked effect due to orientation. Finally, Fig. 7 shows that the carbon may be added after the primary recrystallization structure has formed, with essentially the same result.

In some areas of crystal No. 1 secondary recrystal-lization had begun during the 1 min anneal, and Fig. 8 shows such an area. The secondary shown in the micrograph is clearly more perfect than most of the surrounding primaries. (That the secondary is in deviating orientation from the strong-textured matrix of primaries may also be inferred from the very large angles opposite junctions with boundaries of the primary structure.)

Fig. 9 illustrates a structure selected for a determination of the dislocation density of the primaries of crystal No. 1 after a 1 min anneal at 980°C. In an area of 100 cm^2 at $1000 \times$, there were 2038 pits, giving, therefore, an average dislocation density of 2.0×10^7 lines/cm². One area of 36 mm² contained 32 pits, and thus a density of 9×10^7 lines/cm²; this density may be taken as the upper level found in the present work.

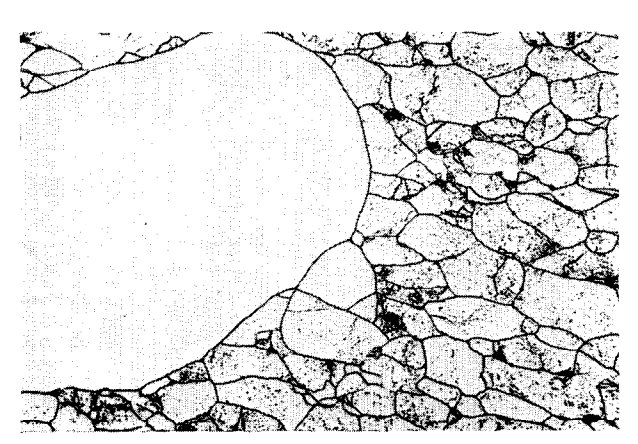


Fig. 8. Microstructure of crystal No. I after a 1 min anneal at 980°C. Different area from Fig. 1. ×500.

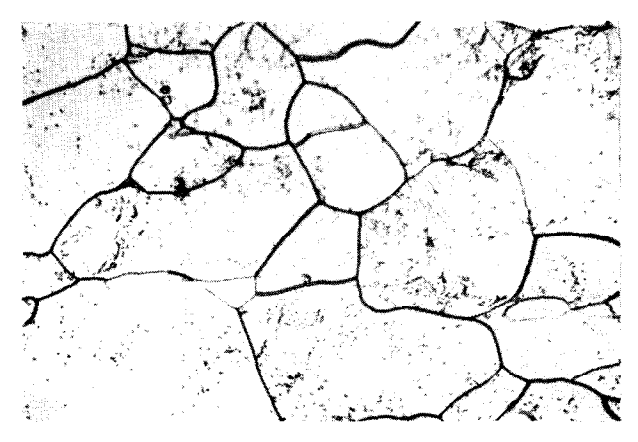


FIG. 9. Typical microstructure of primary recrystallization grains. ×1000.

Fig. 10 illustrates the structure of a secondary in crystal No. 1 after a 30 min vacuum anneal at 980°C which completed secondary recrystallization. The measured density of dislocations in secondaries was $2 \times 10^6 \, \mathrm{lines/cm^2}$; this density is an order of magnitude less than that in the primaries and is about the same as the dislocation density found by Hibbard and Dunn(8) in undeformed silicon-iron crystals.

DISCUSSION

Grain imperfection in terms of disorientation of subgrains

If a Gaussian distribution with half-width, β , is assumed for the orientations of the subgrains, the following relationship between β and the dislocation density, ρ , is obtained.

$$\rho = \beta/(bt\sqrt{2\pi\ln 2})$$

where b is Burgers vector and t is the spacing between subgrain boundaries. The formula is the one derived

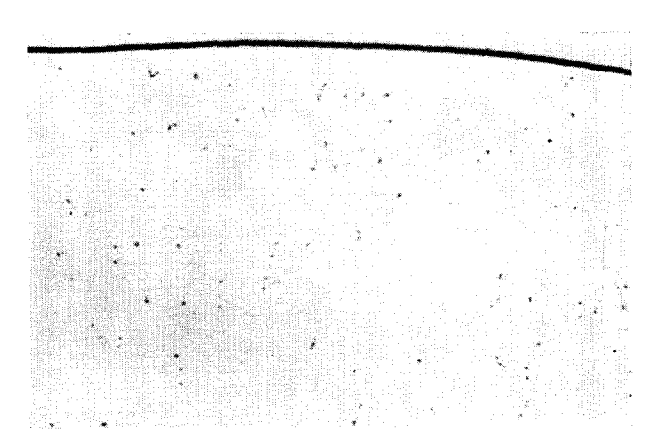


Fig. 10. Typical microstructure of secondary recrystallization grains. $\times 1000$.

by Gay et al.,⁽¹⁰⁾ except for a correction involving the average disorientation which is clarified in the Appendix.

If a random distribution of the dislocations represents the subgrains reasonably well, the above equation can be transformed to give

$$\rho = \beta^2/(2\pi b^2 \ln 2) \simeq \beta^2/(4.35b^2)$$

This relationship is to be contrasted with $\rho = \beta^2/(9b^2)$, which Kurtz *et al.*⁽¹¹⁾ obtained from the equation $\rho \simeq \beta/(3bt)$ of Gay *et al.*

Solving for β in seconds of arc gives

$$\beta = 4.3b \sqrt{\rho} \times 10^5$$

Substituting the values of the dislocation densities found in the present work and using 2.47×10^{-8} cm for Burgers vector gives 48 sec for the half-width of primaries and 15 sec for the half-width of secondaries.

Energy density due to grain imperfections

An energy density, ϵ_d , can be calculated if the energy per unit length of dislocation line is known. Dunn and Aust ⁽¹²⁾ obtained a value of 14×10^{-4} ergs/cm for the energy of a single edge dislocation in Si-Fe when the dislocation density averaged approximately 10^7 lines/cm²; so 14×10^{-4} may be used here provided a volume correction factor of 2 is also used (see ref. 12). The value of ϵ_d^p , for primaries, with a measured density of 2×10^7 lines/cm², accordingly is 5.6×10^4 ergs/cm³, while ϵ_d^s , for secondaries, is 5.6×10^3 ergs/cm³. The difference in energy density, which would be available as a driving force for growth of a secondary is $\epsilon_d^p - \epsilon_d^s$ and this is approximately 5×10^4 ergs/cm³.

Energy density due to boundaries of primaries

If r is the average radius of primaries and if γ is the average specific grain-boundary energy, then the energy density, ϵ_g , due to boundaries is $k \gamma/r$, where k is a geometrical factor near the value 2 (the value 2 will be used hereafter). When, as in the present case, the texture is strong, γ is appreciably below the specific energy of a high-angle boundary, so it becomes necessary to find some reliable estimate of the proper value to take. Following Dunn and Aust, (12) a value of γ_m of 10^3 ergs/cm² will be taken as the specific energy of a high-angle boundary, and, according to the Shockley-Read dependence of energy with angle of misfit, γ_m may be taken as the maximum value reached when the disorientation is 25° .

Dunn^(13, 14) has reported a normal, but bivariate, distribution, for the (110) poles in each isolated pole concentration of the texture. In one instance of a sharp

as-recrystallized texture (which corresponds to the texture of crystal No. 1 of the present work after the I min anneal at 980°C), the standard deviations σ_x and σ_{ν} found were 3.2° and 2.3°, respectively. What is needed here, of course, is the distribution of pairs of poles, since two poles per grain are required to determine each orientation. Lacking this information, let us assume, as Gay et al. (10) do, a Gaussian distribution of the orientations so that each orientation can be referred to a mean position. Thus the probability that the orientation of a given grain will be at an angle θ to the mean orientation will be proportional to $\exp \left(-\frac{\theta^2}{2\sigma^2}\right) d\theta$ and that the orientation of a neighboring grain will be at an angle ϕ will be proportional to exp $(-\phi^2/2\sigma^2) d\phi$. The probability that both grains will be simultaneously at the angles θ and ϕ is, therefore, the product exp $[-(\theta^2 + \phi^2)/2\sigma^2] d\theta d\phi$; this product can be used to obtain an average of the disorientation ($\theta - \phi$) or an average value of γ , provided σ is known. Based on experimental values of σ_x and σ_y near 3° and 2°, respectively, we estimate σ to be approximately 4°. Such a standard deviation corresponds to a half-width of the Gaussian distribution curve of β equal to $\sigma\sqrt{8 \ln 2}$, or 9.4°. Since $|\theta - \phi| = 2\sigma/\sqrt{\pi}$, according to results obtained in the Appendix (see equation 2), the average disorientation is 4.5° .

The variation of the specific energy of a grain boundary with disorientation, according to the Shockley-Read equation⁽¹⁵⁾ and the present terminology, would be

$$\gamma = (\gamma_m/\delta)|\theta - \phi| \ln e\delta/(|\theta - \phi|)$$

where e is the base of natural logarithms and δ is the value of $|\theta - \phi|$ when $\gamma = \gamma_m$. This equation reduces to $\gamma = 0.49 \gamma_m$ at $|\theta - \phi| = 4.5^\circ$, the average angle, and $\delta = 25^\circ$. A direct calculation of $\bar{\gamma}$ gives the following (see derivation of equation 5 in the Appendix).

$$ar{\gamma} = \gamma_m \, 2\sigma/(\delta\sqrt{\pi}) \, \{ \ln \, (e\delta/2\sigma) \, + \, 0.289 \}$$

and this reduces to

$$\bar{\gamma} = 0.44 \, \gamma_m \quad \text{for} \quad \sigma = 4^{\circ} \quad \text{and} \quad \delta = 25^{\circ}.$$

(When σ is sufficiently small, as for example 4°, it can be shown that there is only a negligible contribution to the integral of equation 4 of the appendix for $|\theta - \phi|$ beyond 20°. It follows that the Shockley-Read equation can be used here despite the infinite limits of θ and ϕ .)

The energy density due to grain boundaries becomes

$$\epsilon_g = 2(0.44)\gamma_m/r_p$$
 or $5.9 \times 10^5 \, \mathrm{ergs/cm^3}$

for grains of 15 μ radius and γ_m at 1000 ergs/cm².

Comparison of energy densities from imperfections and grain boundaries

The total energy-density change that occurs when primaries are replaced by one very large secondary is $\epsilon_d{}^p - \epsilon_d{}^s + \epsilon_g$, or $6.4 \times 10^5 \, \mathrm{ergs/cm^3}$. The fraction of the energy density supplied by primaries, therefore, is 8 per cent*. Consequently, the imperfections within primaries, as found here, provide only a small contribution to the driving force for growth of a very large secondary. The situation may, however, be entirely different when secondaries are still small, as they have to be early in the secondary recrystallization process.

The driving force for growth of a secondary, omitting any restraining effect due to inclusions, may be written as follows for the general case:

driving force =
$$\epsilon_d^p - \epsilon_d^s + 2(\gamma/r_p - \gamma_m/r_s)$$

where γ may be taken as 0.44 γ_m . The contribution from imperfections, therefore, will always be positive provided $\epsilon_d^{\ p} > \epsilon_d^{\ s}$; it becomes the main term when r_s is near $2r_{\nu}$. If the grain that grows into a secondary should have the relatively low density of 2×10^6 lines/cm² when it is still one of the primaries (a primary in deviating orientation⁽¹⁶⁾), then the contribution from imperfections can be very important. Using the average density, for example, corresponding to $\epsilon_d^{\ p} - \epsilon_d^{\ s}$ equal to 5×10^4 , 1000 for γ_m , 440 for γ , and 15×10^{-4} for r_p , we find that the grain-boundary term is zero at r_s equal to 34 μ and only becomes equal to the imperfection term at r_s equal to 37 μ . The imperfection term becomes even more important, of course, in small regions where the density of dislocations is appreciably above the average; this term could play an important role in getting the primary (nucleus for secondary recrystallization) up to or substantially beyond the average critical size for growth. In the present example the average critical size would be 31μ , because the average driving force would then be zero.

It seems doubtful that regions surrounding the nucleus for secondary recrystallization would have an average dislocation density as high as our measured upper value of 9×10^7 lines/cm². If this does occur, however, due to local variations, a net driving force for growth arises, according to the above equation, only for potential nuclei above 24 μ radius. Such variations would have an even greater effect, however, on initiating growth of the larger nuclei for secondary recrystallization. In any case, the present results indicate that the conclusion reached by Dunn⁽¹⁶⁾

(namely, that the size of the primaries, which become secondaries, must be two to three times the average size of primaries) is still essentially correct for structures of the type encountered in the present work.

Origin of imperfections within primaries

No serious effort has been made in the present work to determine the origin of the dislocations within primaries or even to determine whether or not certain primaries are more perfect than others, since this effort would involve obtaining the three-dimensional structure. The single-section view of the present work, for example, indicates that some primaries have relatively low dislocation densities (edge-type), but other sections taken through the same primaries might reveal higher-density regions. If early-forming primaries become strained⁽⁶⁾ due to release of internal stresses during recrystallization in the manner suggested by Polanyi and Sachs, (17) then such primaries could be expected to have higher dislocation densities than later-forming primaries. If the nucleus for primary recrystallization is rather imperfect, (6) as suggested by Snoek, (18) then one might expect most of the primaries to be imperfect. Further experiments are expected to throw light on this subject.

CONCLUSION

Based on measured differences in dislocation densities, the grains in fine-grained structures of silicon-iron obtained by primary recrystallization are less perfect than the secondary recrystallization grains that replace them on further annealing. The imperfections are considered capable of providing an important driving force during the early stages of secondary recrystallization, while the contribution to the driving force tends to be negligible when the secondaries become large.

ACKNOWLEDGMENTS

The authors thank Dr. R. H. Pry and Dr. W. R. Hibbard Jr. for discussions and critical reviews of the manuscript, and Dr. G. M. Roe for help in obtaining equation (5) given in the Appendix of the paper.

Appendix

Average disorientation

The method of Gay et al. $^{(10)}$ for calculating the average disorientation is given in equation (1).

$$|\theta - \phi| = \frac{\int_{-\infty}^{\infty} \int_{-\infty}^{\infty} |\theta - \phi| \exp\left[-(\theta^2 + \phi^2)/2\sigma^2\right] d\theta d\phi}{\int_{-\infty}^{\infty} \int_{-\infty}^{\infty} \exp\left[-(\theta^2 + \phi^2)/2\sigma^2\right] d\theta d\phi}$$
(1)

^{*} In this calculation it is clear that the per cent contribution is independent of the value taken for γ_m , because γ_m cancels out in the ratio.

The denominator has the value $2\pi\sigma^2$. According to Pry, (19) the numerator can be integrated explicitly using the following method. Let x equal $\theta - \phi$ for $\phi < \theta$ and x' equal $\phi - \theta$ for $\phi > \theta$. Substitution gives two terms with limits 0 and ∞ for x and x'. The distinction between x and x', may be dropped because of the infinite limits and the terms collected to give

$$\begin{split} \int_{-\infty}^{\infty} \int_{0}^{\infty} x \exp\left(-\theta^2/2\sigma^2\right) \left\{ \exp\left[-\left(\theta^2 - 2\theta x + x^2\right)/2\sigma^2\right] \right. \\ \left. + \exp\left[-\left(\theta^2 + 2\theta x + x^2\right)/2\sigma^2\right] d\theta \, dx \end{split}$$

According to standard forms, this integral has the value $4\sigma^3 \sqrt{\pi}$. Equation (1), therefore, reduces to

$$|\overline{\theta - \phi}| = 2\sigma/\sqrt{\pi}. \tag{2}$$

The relationship between the standard deviation, σ , and the half-width, β , of the Gaussian distribution curve is

$$\sigma = \beta/(2\sqrt{2 \ln 2}).$$

Therefore

$$|\theta - \phi| = \beta/\sqrt{2\pi \ln 2} \tag{3}$$

The average angle is, therefore, approximately $\frac{1}{2}\beta$ instead of $\frac{1}{3}\beta$, as found by Gay et al. (10)

An alternate explicit solution can be obtained by noting that the integration of the numerator over the four quadrants in θ and ϕ gives

$$\begin{split} 2 \int_0^\infty \int_0^\infty (\theta + \phi) \exp\left[-(\theta^2 + \phi^2)/2\sigma^2\right] d\theta \, d\phi \\ + 2 \int_0^\infty \int_0^\infty \left|\theta - \phi\right| \exp\left[-(\theta^2 + \phi^2)/2\sigma^2\right] d\theta \, d\phi \end{split}$$

The first term has the value $2\sigma^3\sqrt{2\pi}$, and from it one obtains the numerical integration value of Gay et al., since $2\sigma^3\sqrt{2}\pi/2\pi\sigma^2 = 2\sigma/\sqrt{2\pi} = \beta/(2\sqrt{\pi \ln 2}) = 0.34\beta$.

The second term can also be evaluated explicitly after changing from rectangular to cylindrical co-ordinates. The transformation gives

$$2\int_0^{\pi/2}\int_0^\infty r(|\cos w - \sin w|) \exp(-r^2/2\sigma^2) dw r dr$$

which reduces to $4\sigma^3\sqrt{\pi} - 2\sigma^3\sqrt{2\pi}$. Combining the two results gives $4\sigma^3\sqrt{\pi}$, which is the result obtained above.

The average grain-boundary energy

Using the Shockley-Read equation to define γ in terms of $|\theta - \phi|$, one obtains the following equation for the average value of γ .

$$\bar{\gamma} = (\gamma_m/\delta) - \frac{\int_{-\infty}^{\infty} \int_{-\infty}^{\infty} |\theta - \phi| \ln (e\delta/|\theta - \phi|)}{\int_{-\infty}^{\infty} \int_{-\infty}^{\infty} \exp\left[-(\theta^2 + \phi^2)/2\sigma^2\right] d\theta d\phi}$$
(4)

Omitting the factor γ_m/δ , Pry's method applied to the numerator gives the following:

$$4\sigma^3\sqrt{\pi}\ln{e\delta}=2\sigma\sqrt{\pi}\int_0^\infty x\exp{(-x^2/4\sigma^2)}$$
 . $\ln{x}\,dx$.

With a change in variable this becomes

$$4\sigma^3\sqrt{\pi}\ln\left(e\delta/2\sigma\right) - 8\sigma^3\sqrt{\pi}\int_0^\infty\!\!y\,\exp\left(-y^2\right).\ln y\,dy.$$

However,

$$\int_0^\infty y \exp{(-y^2)} \cdot \ln y \, dy = -\frac{0.5772...}{4}...$$

the number (-0.5772...) being Euler's constant E. Equation (4), therefore, reduces to

$$\bar{\gamma} = \gamma_m 2\sigma/(\delta\sqrt{\pi}) \left\{ \ln\left(e\delta/2\sigma\right) - E/2 \right\}$$
 (5)

REFERENCES

- 1. W. G. Burgers Rekristallisation, Verformter Zustand und Erholung. In Masing Handbook der Metallphysik Vol. III. p. 2. Leipzig (1941); also Edward Brothers, Ann Arbor, Michigan (1944).
- C. S. BARRETT The Structure of Metals (2nd edition) McGraw-Hill, New York (1952).
- J. E. BURKE and D. TURNBULL Progr. Metal Phys. 3, 220
- W. G. Burgers L'état solide p. 73. Brussels, Institute International de Physique (1951)
- P. A. BECK Adv. Phys. 3, 245 (1954).
 G. W. RATHENAU and J. F. H. CUSTERS Philips Res. Rep. **4**, 241 (1949).
 A. Guinier and J. Tennevin Philips Res. Rep. **4**, 318
- (1949).
- W. R. HIBBARD, JR. and C. G. DUNN Acta Met. 4, 306
- J. C. Suits and J. R. Low Acta Met. 5, 285 (1957).
- 10. P. GAY, P. B. HIRSCH, and A. KELLY Acta Met. 1, 315,
- A. D. Kurtz, S. A. Kulin, and B. L. Averbach Phys. Rev. 101, 1285 (1956).C. G. Dunn and K. T. Aust Acta Met. In press.
- 13. C. G. DUNN Acta Met. 2, 173 (1954).
- C. G. DUNN J. Appl. Phys. 25, 233 (1954).
 W. SHOCKLEY and W. T. READ Phys. Rev. 78, 275 (1950).
- 16. C. G. Dunn Acta Met. 1, 163 (1953).
- 17. M. POLANYI and G. SACHS Z. Metallk. 17, 227 (1925).
- J. L. Snoek See reference 1. page 246.
- 19. R. H. PRY Private communication.